

Surface Microstructure and Anti-wear of WC-CoCr Coatings Cladded by Electron Beam

Liu Hailang^{1,2}, Wang Bo², Qi Zhengwei², Zhang Guopei², Wang Dezhi¹

¹ Central South University, Changsha 410073, China; ² Guilin University of Electronic Technology, Guilin 541004, China

Abstract: Nickel based alloy has good corrosion resistance in chloride medium, but its wear resistance is insufficient. In this paper, WC-CoCr coatings were deposited on Inconel617 alloy surface by HVOF (high velocity oxygen fuel). Electron beam remelting process was explored to modify the morphology and the phase composition of the coated layer. The results show that some structural defects of the as-sprayed coating are improved after electron beam treatment. Tribological tests concerning the sliding wear behavior of the tested materials reveal a significant decrease in the wear rate for the alloyed surface in comparison with the base material. After high energy electron beam treatment, the micro-hardness ($HV_{0.3}$) of the surface is 11000 MPa which is about 2 times as much as that of the matrix (5500 MPa) due to the formation of new phase (especially the Co_6W_6C phase) with high hardness. Besides the amount of porosity of the coatings is reduced and the grain is refined. EDS spectrum analysis indicates that new elements occur in the proliferation of cladding layer and the substrate achieves a good metallurgical bonding with the coating. Moreover, the corrosion resistance of the cladding layer in salt water is higher than that of the matrix.

Key words: electron beam cladding process; WC-CoCr; wear resistance; Inconel617 alloy

Inconel617 is a kind of nickel-base superalloy. It still possesses excellent corrosion resistance even under the condition of hundreds of degrees higher than the working temperature. Nevertheless, the poor wear resistance has a great effect on the application of Inconel617^[1,2]. Therefore, it is very important to improve wear resistance of Inconel617 for practical applications.

One effective route for improving the wear resistance is achieved by exerting the tungsten carbide coatings. In the various categories of coating material, WC-CoCr coating featured by its high hardness and good corrosion-resistance causes more interests for the aerospace, automotive, transportation and power generation systems industries applications^[3-5]. The differences in coating technologies are attributed to variation of coatings microstructures and consequently the coating properties^[6]. From the group of thermal spraying technologies, the High Velocity Oxygen Fuel (HVOF) technology is usually used to deposit the ceramic coatings^[7-9]. However, the WC-CoCr coating fabricated directly by HVOF technique al-

ways has the inherent shortcomings, such as non-bonded interfaces, buried porosities and micro-cracks, which shorten the service time of coating system. On the other hand, electron beam (EB) surface cladding process, one of the most efficient and versatile techniques, can improve the wear resistance and hardness of WC-CoCr coatings on Inconel617 alloy. As compared to laser and ion beam techniques, the EB has been developed rapidly in recent years and shows substantial potentials in surface treatment engineering for its deeper modified layer of hundreds of micrometers and high efficiency of energy absorption up to ~80%. The adhesion strength between WC-CoCr coatings and Inconel617 base can be enhanced by EB treatment. Moreover, the grains in the coatings are finer, and the coating surface is more homogeneous and denser^[10-13]. In this paper, the EB irradiation of sprayed WC-CoCr coating was carried out with optimal parameters. By applying this treatment, the coating porosity and possible microcracks or internal oxides might be reduced^[14-16] and, the chemical composition might be improved especially with respect to Cr and

Received date: November 15, 2017

Foundation item: Innovation Project of GUET Graduate Education (2017YJXC14)

Corresponding author: Wang Bo, Master, School of Mechanical and Electrical Engineering, Guilin University of Electronic Technology, Guilin 541004, P. R. China, E-mail: 1215732707@qq.com

Copyright © 2018, Northwest Institute for Nonferrous Metal Research. Published by Elsevier BV. All rights reserved.

Mo-content, the latter one being responsible for a good corrosion resistance in salt water^[17-19]. In the present work, the surface microstructure, distribution of chemical composition and the phase composition would be investigated before and after EB treatment. Sliding wear resistance and the corrosion resistance of the refined surface were compared with those of Inconel617 alloy substrate. The surface microhardness of the samples before and after EB treatment was also determined^[20,21].

1 Experiment

The WC-CoCr coating (powder size of 21~50 μm and nominal composition of 88wt% WC, 8wt% Co, 4wt% Cr) were deposited on Inconel617 alloy substrate of size $\Phi 30\text{ mm} \times 6\text{ mm}$ by PTA-400E1-600V type thermal spraying system. The coating thickness was $\sim 500\text{ }\mu\text{m}$. The process pa-

rameters of HVOF for the WC-CoCr coatings are as follows: air pressure 0.7 MPa, oxygen pressure 1.0 MPa and flow 1100 L/min, propane pressure 0.6 MPa and flow 1100 L/min, powder feeding mode nitrogen feeding powder and powder feeding pressure 0.9 MPa. The chemical composition of the Inconel617 is shown in Table 1.

The electron beam irradiation was carried out at Guilin University of Electronic Technology of China with a THDW type EB apparatus, which included melting gun, welding gun, scanning gun and electron beam zone melting gun. Electron beam surface treatment was carried out in vacuum by the EB scanning gun with a maximum beam input power of 6 kW. Detailed parameters of EB remelting for the WC-CoCr coatings are shown in Table 2.

Table 1 Chemical composition of Inconel617 (wt%)

Element	Ni	Cr	Fe	C	Mn	Si	Mo	Co	Al	Ti	P	S
Min.	Bal.	20	-	0.05	-	-	8.0	10.0	0.6	0.2	-	-
Max.	Bal.	23	2.0	0.1	0.7	0.7	10.0	13.0	1.5	0.6	0.012	0.008

Table 2 Experimental parameters for EB remelting

Parameter	Value
Accelerating voltage/kV	50
EB current/mA	60
Focusing current/mA	350
Scan speed/mm·min ⁻¹	1000
Scan frequency/Hz	500

The sliding wear resistance was tested using MPX-2000 pin-on-disk friction and wear tester. SiC balls with a diameter of 6 mm were used as a counterpart (pin), the speed v was 500 r/min, and the testing distance 1000 m (the radius of the sliding path was 5 mm). The weight of the sample was measured every 1 h by AR2130 electronic balance. The X-ray diffraction technique was performed on a D8ADVANCE diffractometer using Cu K α radiation in order to determine the phase modification. The data were collected by applying 2θ values in the range of $20^\circ \sim 100^\circ$. The surface microstructure was observed by tension optical microscopy (OM) and Quanta 450 FEG scanning electron microscope (SEM). The chemical composition was measured on the cross-section of sample using energy dispersive system (EDS). Micro-hardness measurement of cladding layer to matrix cross section was carried out by HV-1000 micro-hardness tester.

Corrosion experiments were carried out at room temperature. The sample was soaked in 3.5% NaCl solution for 3 h, and its polarization curve was observed. The corrosion potential E_{corr} and corrosion current density i_{corr} were calculated by Tafel linear extrapolation method. The corrosion resistance of the cladding layer of Inconel617 alloy after

electron beam scanning was also analyzed.

2 Results and Discussion

Fig.1 gives the general aspects of sprayed WC-CoCr coating. Large cavities and micro-cracks were observed on the surface of the coating as shown in Fig.1a. The mode of the bonding between substrate and ceramics coating is mainly mechanical bonding. At the junction between the coating and the substrate is a gray gap with obvious macroscopic defects and the gap probably derived from the sample cutting or metallographic preparation process due to the adhesion between matrix and coating is insufficient, as shown in Fig.1b. The bond strength between coating and substrate is one of the most important targets to satisfy the mechanical, physical and chemical properties for coatings in application.

Fig.2 shows SEM images of the surface electron beam treated WC-CoCr coatings. Under electron beam irradiation, both the coating and the substrate were first melted and intermixed, and then rapidly solidified, forming a new alloyed surface^[22,23]. It can be seen that the sprayed coating is modified ultimately, and the shape of grains is varied, such as dendritic and chain structure, as shown in Fig.2a. The mode of the bonding between substrate and ceramics coating becomes fully metallurgical bonding (Fig.2b). Also, it can be seen a small amount of micropores but there are no micro-cracks in the cladding layer. It demonstrates the microstructure of the coating is improved to a certain extent after EB treatment.

EDS was conducted on the cross-section of coating with a map scanning mode. Fig.3 shows the EDS results of sprayed WC-CoCr coating. The main part of coating is

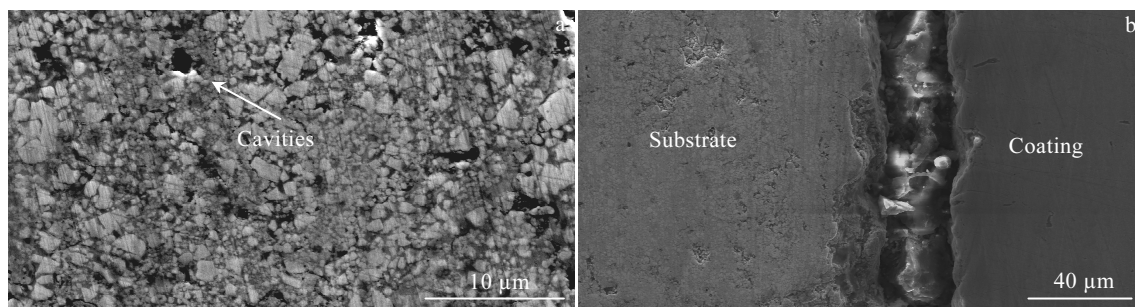


Fig.1 Morphologies of as-sprayed WC-CoCr coating: (a) surface and (b) cross-sectional

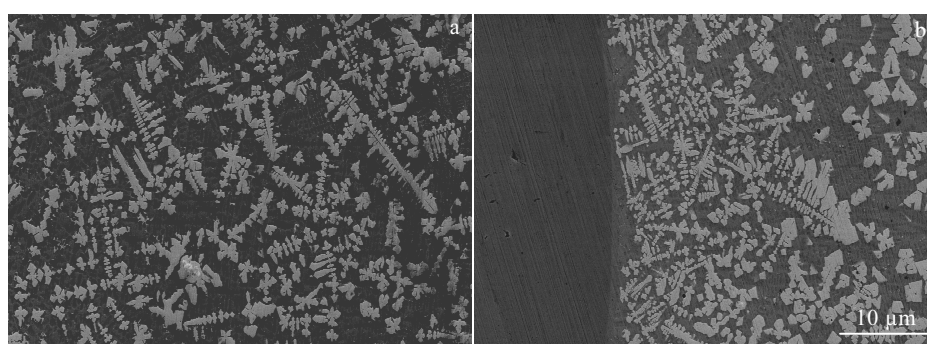


Fig.2 SEM images of the coating after EB-remelting: (a) upper region and (b) interface of coating/substrate

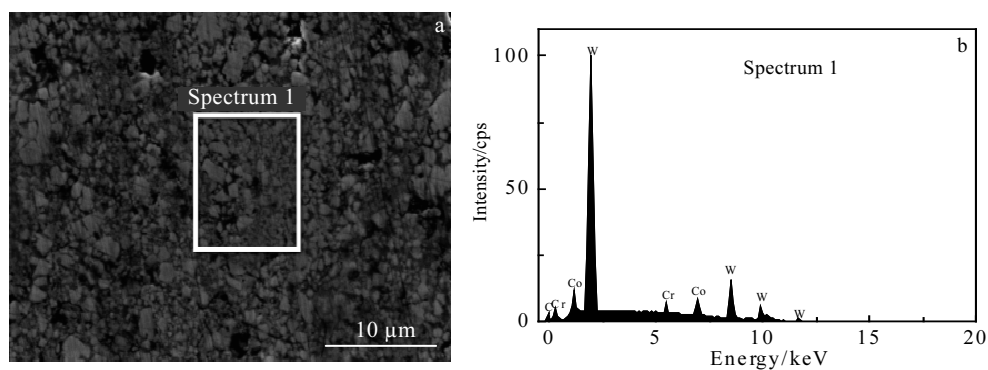


Fig.3 SEM image (a) and EDS spectrum (b) of as-sprayed coating

composed of W and C elements. The content of Co and Cr in coating is 12.7%. The typical EDS analysis of EB-treated WC-CoCr coating are shown in Fig.4. The W and C elements are uniformly distributed in the remelted layer. The new elements of Fe, Mn and Ni are found in the remelted coating. EDS spectrum analysis indicates that the process of electron beam cladding elements occur in the proliferation of cladding layer and the substrate achieves a good metallurgical bonding with the coating.

The composition of EB remelted coating in spectrum 3 in Fig.4a was tested by EDS, and it is found that the spectrum 1 (dendritic zone) in Fig.4a is mainly composed of W ele-

ment. Co and Cr elements are in the majority in spectrum 2 (gray zone) in Fig.4a. Due to the rapid cooling characteristics during the electron beam treatment, the rich tungsten phase forms a specific dendrite in the cooling process and uniformly distributes in the CoCr matrix.

Through XRD pattern analysis, the phase composition of sprayed WC-CoCr coating is mainly WC and W_2C ; W_2C is due to decomposition of WC during high temperature spraying, and Co_2C occurs due to partial carbonation of CoCr phase, as shown in Fig.5a. At high temperature, a few reactions have happened as follows:

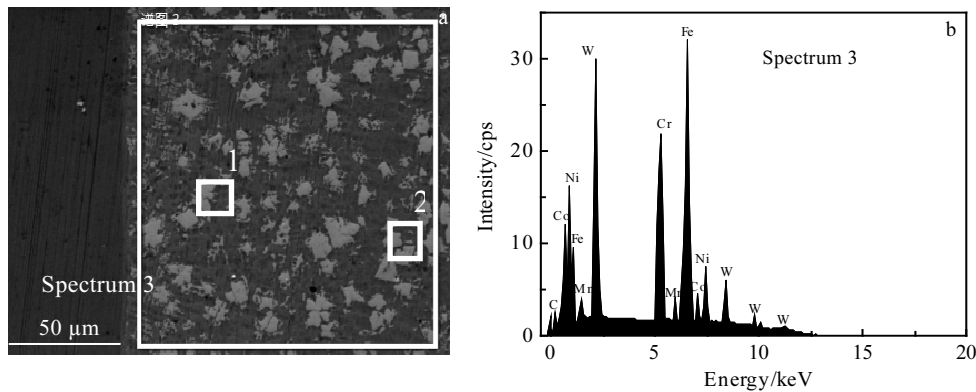


Fig.4 SEM image (a) and EDS spectrum (b) of EB remelted coating

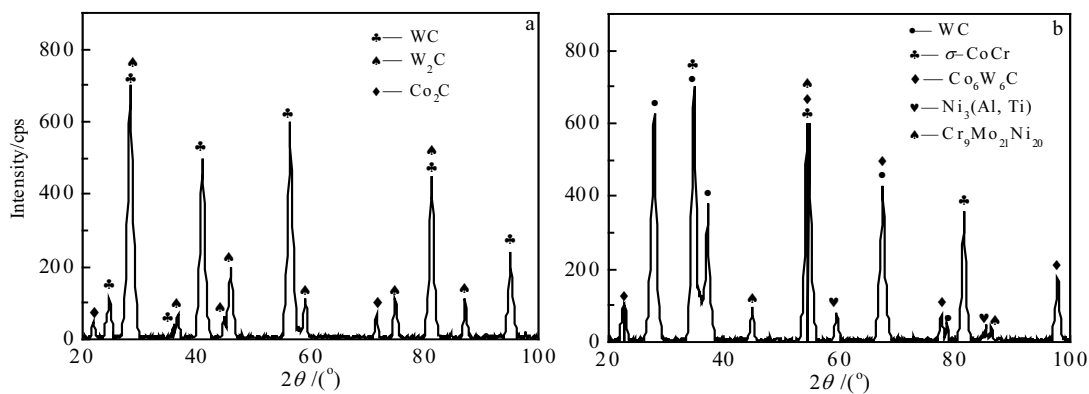


Fig.5 XRD patterns of as-sprayed coating (a) and EB remelted coating (b)



The CoCr phase did not appear in the spectrum because the ratio between WC and CoCr in WC-CoCr powder is highly different while the content of WC is as high as 88%.

After high energy electron beam treatment, in addition to the original phase WC, σ -CrCo occurs in the cladding layer, new phase $\text{Co}_6\text{W}_6\text{C}$, $\text{Ni}_3(\text{Al}, \text{Ti})$ and $\text{Cr}_9\text{Mo}_{21}\text{Ni}_{20}$ are formed, as shown in Fig.5b. The high temperature environment during electron beam scanning results in the formation of composite carbide. Among them, double carbide $\text{Co}_6\text{W}_6\text{C}$ has higher hardness than WC, and it is the main phase structure in improving the hardness and wear resistance of the cladding layer. Due to the presence of Co, the toughness of the hard phase is also improved to some extent. $\text{Ni}_3(\text{Al}, \text{Ti})$ is a typical γ' phase in nickel based alloys. It is the second phase precipitated from supersaturated solid solution, which is a face centered cubic structure, and the lattice constant is similar to that of the matrix and is identical with that of crystal. Therefore, the γ' phase can precipitate

evenly in small particles and hinder dislocation movement, resulting in significant strengthening action. Moreover, the presence of Co in the coating improves the intensity of the γ' phase. Inconel617 alloy is mainly used in aviation turbine parts and high temperature pipelines. These working conditions require very high resistance to materials oxidation. After the electron beam processing of WC-CoCr, the $\text{Ni}_3(\text{Al}, \text{Ti})$ containing Ni and Al elements can greatly improve the high-temperature oxidation resistance of the sample surface and adapt to a variety of oxidation environment. $\text{Cr}_9\text{Mo}_{21}\text{Ni}_{20}$ containing Mo element has higher pitting corrosion resistance and can improve the corrosion resistance of the alloy.

Micro-hardness test on the substrate and cladding layer (Fig.6) shows that after the electron beam treatment, the reinforcing phase and micro-structure are evenly distributed in the cladding area and the micro-hardness of the cladding layer fluctuates little. The highest hardness ($\text{HV}_{0.3}$) is 11 000 MPa which is about 2 times higher than that of the substrate. The micro-hardness of the cladding surface to the transition layer shows a trend of rising.

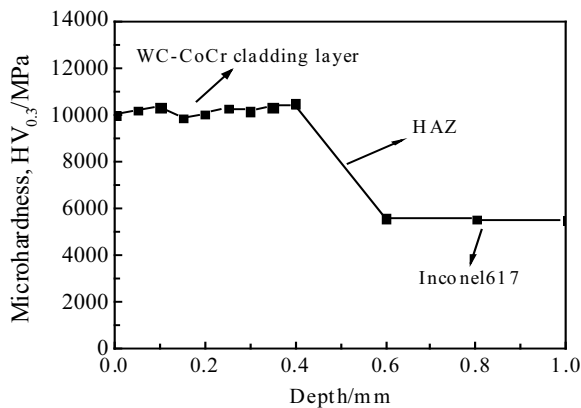


Fig.6 Micro-hardness vs depth curve of the WC-CoCr coating after EB-alloying

The reason is that WC-CoCr does not appear to be floating during the process of electron beam cladding, and the elements of hard phase such as W, C slowly move towards the substrate when they are exchanged with the elements of substrate. In the maximum micro-hardness of cladding layer, it is assumed that the phases are dendrites of WC and $\text{Co}_6\text{W}_6\text{C}$. Also, it possibly contains γ' phase which is the second enhancement phase. For the Inconel617 alloy substrate, the micro-hardness of the matrix is decreased with the increase of the distance between the alloy and the interface. The micro-hardness is higher when it is closer to the interface. The main reason is that the process of electron beam remelting is equivalent to the quenching of the surface of Inconel617 alloy. But the micro-hardness of the matrix is not very different.

Fig.7 presents the wear surface topography of Inconel617 alloy matrix and the cladding layer. It can be seen that SiC causes the severe ploughing to surface of Inconel617 alloy, and a deep groove and adhesive wear occurs (Fig.7a) since to Inconel617 alloy is soft itself. WC and $\text{Co}_6\text{W}_6\text{C}$ hard phases are formed as a framework in the cladding layer after the electron beam treatment and other elements are evenly distributed in this framework. Thus the specimen is protected during the process of friction and wear due to existence of WC and $\text{Co}_6\text{W}_6\text{C}$ hard phase which hinder the cutting action of SiC on the surface of the cladding layer. We can see a relatively smooth wearing surface as shown in Fig.7b. Under the cyclic friction of SiC, it has a severe ploughing effect on the softer CoCr phase in the cladding at first. The hard phase of WC and $\text{Co}_6\text{W}_6\text{C}$ gradually emerges with the process of friction and wear, and improves the wear resistance of the specimens. These results indicate that WC-CoCr decomposed into W, C and other elements in the molten pool during the irradiation of electron beam forms a new hard phase to effectively strengthen the micro-structure of cladding layer.

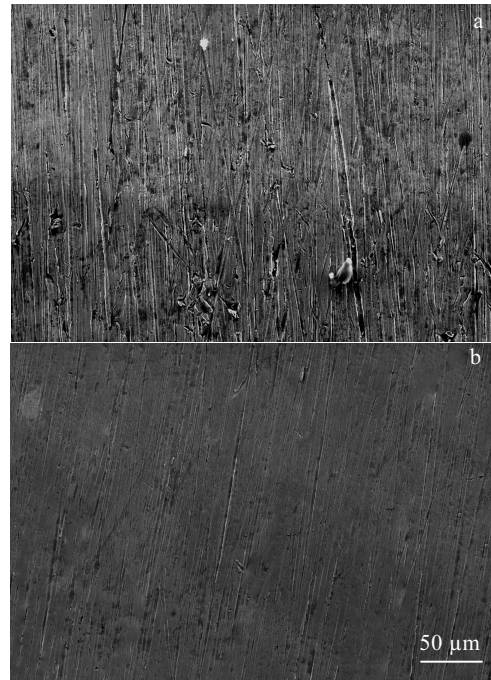


Fig.7 Surface morphologies of Inconel617 alloy (a) and the WC-CoCr coating after EB-alloying (b)

Fig.8 shows the sliding wear histogram of the tested specimens. The wear rate of the remelted coating is about 4 times lower than that of the Inconel617 substrate. The increase of cladding layer wearing resistance is an effective guarantee for the overall performance. Moreover, the interface between large WC particles and Inconel617 alloy forms a reaction layer of several hundred microns which enhances the toughness of interface highly.

Fig.9 shows the relationship between abrasive weight loss and experiment time. The WC-CoCr cladding layer shows significantly less weight loss than that of the Inconel617 substrate. If reciprocal of wear loss represents the wear resistance, the wear resistance of cladding layer in

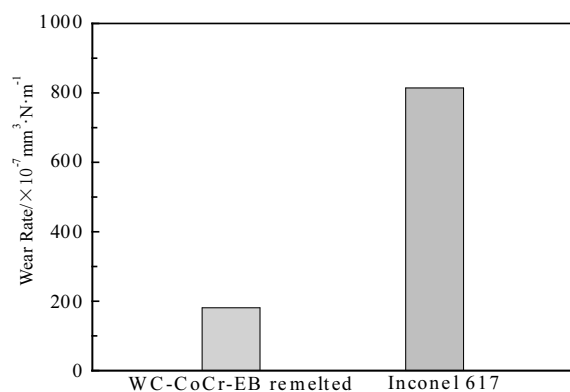


Fig.8 Sliding wear rate of the WC-CoCr coating after EB-alloying

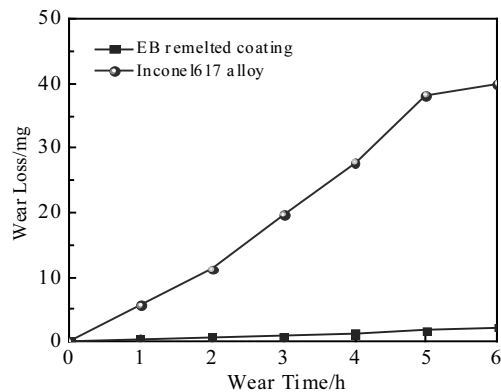


Fig.9 Results of sliding wear test

creases by over 10 times comparing with Inconel617 alloy. The reason is that WC-CoCr coating layer and Inconel617 alloy substrate exchange ions each other after high energy electron beam treatment, then forming a fine metallurgy combination and making cladding layer not easy to drop.

The corrosion potential reflects the thermodynamic tendency of corrosion. Under a certain medium condition, the corrosion potential is a fixed value. It is that the lower the corrosion potential value, the greater the possibility of corrosion of the material. The corrosion current density reflects the dynamic characteristics of the corrosion process. Generally speaking, the higher the anodic polarization current density is, the higher the corrosion rate is.

As illustrated in Fig.10 and Table 3, the corrosion potential of untreated WC-CoCr coating is -0.702 V and the corrosion potential is -0.472 V after electron beam treatment. The corrosion potential moved forward obviously. The corrosion current density of the untreated WC-CoCr coating is $1.735 \times 10^{-5} \text{ A/cm}^2$, and that after electron beam cladding is only $2.624 \times 10^{-6} \text{ A/cm}^2$, which is reduced by an order of magnitude. It shows that the corrosion resistance of WC-CoCr ceramic coating is greatly improved by electron beam cladding. The corrosion current density of Inconel617 alloy in 3.5% NaCl solution is $7.153 \times 10^{-6} \text{ A/cm}^2$ which is larger than that of the cladding layer, but their difference is little. It shows that the corrosion resistance of cladding is slightly better than that of Inconel617 alloy. The reason is that the WC-CoCr coating itself contains Cr element with excellent corrosion resistance and during the corrosion process, a small amount of chromium was added to the CoCr binder phase to form a chromium oxide passive film which can avoid the micro galvanic corrosion between the WC particles and the bonding phase. After the electron beam treatment, the addition of Ni and Mo elements with good corrosion resistance and the homogeneous distribution of Cr rich phases in the matrix are also the main reason for the increase of corrosion resistance of cladding layer. The

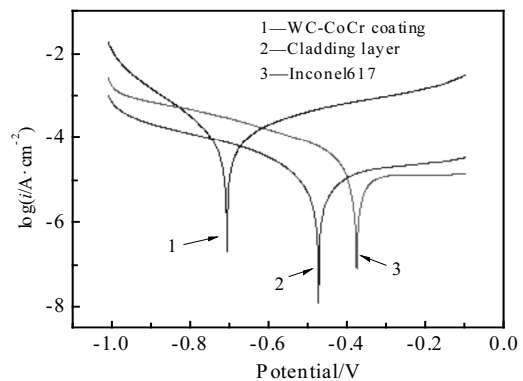


Fig.10 Polarization curves of electrochemical corrosion

Table 3 Electrochemical corrosion characteristics data

Material	E_{corr}/V	$i_{\text{corr}}/\times 10^{-6} \text{ A}\cdot\text{cm}^{-2}$
Inconel617	-0.375	7.153
Cladding layer	-0.472	2.624
WC-CoCr coating	-0.702	17.35

performance of the corrosion depends largely on the elements of the material itself and on the composition of the elements^[24]. Some elements (such as Co, Cr, Mn, Al, etc) can improve the corrosion resistance of the material because they react with the corrosion elements to produce a dense passive film. Inconel617 alloy has higher corrosion resistance because it contains higher concentrations of Co, Cr and other elements which can improve corrosion resistance. WC-CoCr coating has a certain degree of corrosion resistance, but content of corrosion resisting elements is lower than that of Inconel617 alloy. However, after high energy electron beam treatment, the ion exchange between coating and substrate is achieved to improve the corrosion resistance of coating while the ion exchange between coating and substrate for the WC-CoCr coatings does not be achieved in the process of HVOF. Moreover, the molecular structure of the coatings is not changed by HVOF spraying and there is still a gap in the powder coating. The presence of gaps do not prevent the entry of corrosive elements. Therefore, the corrosion rate of the as-sprayed WC-CoCr coating is the highest.

3 Conclusions

1) Electron beam cladding process of WC-CoCr coatings on Inconel617 alloys has been carried out to study the effect of the electron beam cladding process on the structure and properties of the coatings. SEM examination of the samples in cross-section reveal that the coating surface becomes denser and the shape of grains is varied after EB treatment.

2) The microspores and micro-cracks which appear in the HVOF are reduced or eliminated. After the EB treatment,

the mode of the bonding between substrate and ceramics coating becomes fully metallurgical bonding and new elements such as Fe, Mn, and Ni appear in WC-CoCr coating. The rich tungsten phase forms a specific dendrite and uniformly distributed in the CoCr matrix.

3) The coating demonstrates formation of new phases ($\text{Co}_6\text{W}_6\text{C}$, $\text{Ni}_3(\text{Al}, \text{Ti})$ and $\text{Cr}_9\text{Mo}_{21}\text{Ni}_{20}$), especially $\text{Co}_6\text{W}_6\text{C}$, as well as an enrichment in σ -CoCr, both contributing to a better wear behavior of this sample.

4) EB treatment provides a good route for improving the surface wearing resistance. The wear loss and wear rate decrease obviously after EB remelting, which mainly comes from a mixture of several elements. Moreover, after electron beam cladding of WC-CoCr coating, the corrosion current density is only $2.624 \times 10^{-6} \text{ A/cm}^2$. It also has excellent corrosion resistance and can adapt to all kinds of working environments.

5) One should consider the improvement in the sliding wear resistance of this refined surface in comparison with that of as-sprayed coating.

References

- Vilasi M, Francois M, Podor R et al. *Journal of Alloys and Compounds*[J], 1998, 264(1-2): 244
- El-Awadi G A, Abdel-Samad S, Elshazly E S. *Applied Surface Science*[J], 2016, 378: 224
- Hong S, Wu Y, Wang B et al. *Ceramics International*[J], 2017, 43(1): 458
- González M A, Rodríguez E, Mojardín E et al. *Wear*[J], 2017, s(376-377): 595
- Moskowitz L, Trelewicz K. *Journal of Thermal Spray Technology*[J], 1997, 6(3): 294
- Šárka Houdková, Pala Z, Smazalová E et al. *Surface & Coatings Technology*[J], 2016, 318: 129
- Du P C, Zhu X P, Meng Y et al. *Surface & Coatings Technology*[J], 2016, 309: 663
- Li C J, Yang G J. *International Journal of Refractory Metals & Hard Materials*[J], 2013, 39: 2
- Xie M, Zhang S, Li M. *Applied Surface Science*[J], 2013, 273: 799
- He J, Wang S. *Rare Metal Materials and Engineering*[J], 2011, S4: 231
- Tseng S F, Hsiao W T, Huang K C et al. *Surf Coat Technol*[J], 2010, 205(7): 1979
- Miao S M, Lei M K. *Nuclear Inst & Methods in Physics Research B*[J], 2006, 243(2): 335
- Proskurovsky D I, Rotshtein V P, Ozur G E et al. *Surf Coat Technol*[J], 2000, 125(1): 49
- Hamatani H, Miyazaki Y. *Surface & Coatings Technology*[J], 2002, 154(2): 176
- Zhang D, Harris S J, McCartney D G. *Materials Science & Engineering A*[J], 2003, 344(1-2): 45
- Monticelli C, Frignani A, Zucchi F. *Corrosion Science*[J], 2004, 46(5): 1225
- Godoy C, Lima M M, Castro M M R et al. *Surface & Coatings Technology*[J], 2004, 188(1): 1
- Cho J E, Hwang S Y, Kim K Y. *Surface & Coatings Technology*[J], 2006, 200(8): 2653
- Bolelli G, Giovanardi R, Lusvarghi L et al. *Corrosion Science*[J], 2006, 48(11): 3375
- Mateos J, Cuetos J M, Fernández E et al. *Wear*[J], 2000, 239(2): 274
- Lekatou A, Sfikas A K, Karantzas A E et al. *Corrosion Science*[J], 2012, 63(5): 193
- Valkov S, Petrov P, Lazarova R et al. *Applied Surface Science*[J], 2016, 389: 768
- Lenivtseva O G, Bataev I A, Golkovskii M G et al. *Applied Surface Science*[J], 2015, 355: 320
- Li S, Gao B, Yin S et al. *Applied Surface Science*[J], 2015, 357: 2004

电子束熔覆 WC-CoCr 涂层的表面结构及耐磨性研究

刘海浪^{1,2}, 王 波², 祁正伟², 张国培², 王德志¹

(1. 中南大学, 湖南 长沙 410073)

(2. 桂林电子科技大学, 广西 桂林 541004)

摘 要: 镍基合金在含氯介质中有着优异的耐蚀性能, 但其耐磨性不足。利用 HVOF 在 Inconel617 基体上沉积 WC-CoCr 涂层, 研究了经过电子束重熔获得新的改性层, 采用 SEM、EDS 分析改性层的表面形貌以及相成分。结果表明: 经电子束处理后, 一些喷涂层的结构缺陷得到了改善, 涂层空隙减少, 晶粒得到了细化, 由于生成了高硬度的新相 (尤其是 $\text{Co}_6\text{W}_6\text{C}$ 相), 熔覆层的显微硬度 ($\text{HV}_{0.3}$) 为 11000 MPa, 是基体显微硬度 ($\text{HV}_{0.3}$) (5500 MPa) 的 2 倍; 通过摩擦磨损实验分析, 试样相比于基体的滑动磨损行为, 其磨损率显著降低; 而 EDS 分析表明, 熔覆层内出现了新的元素, 基体与涂层达到了良好的冶金结合。此外, 熔覆层在盐水中的抗腐蚀能力有所提高。

关键词: 电子束熔覆; WC-CoCr; 耐磨性; Inconel617 合金

作者简介: 刘海浪, 女, 1978 年生, 博士生, 副教授, 桂林电子科技大学, 广西 桂林 541004, E-mail: 123529746@qq.com